n_H	number of enthalpy-of-mixing experimental points
T	temperature, K

Greek Letters

ρ	density, kg·m^{-3}
ϕ	objective function, eq 3
σ	root-mean-square deviation between calculated and experimental values
η	residual, eq 3

Registry No. 1,3-Dioxolane, 646-06-0; acetic acid, 64-19-7.

Literature Cited

(1) Francesconi, R.; Comelli, F. *J. Chem. Eng. Data* **1985**, *30*, 460.
(2) Francesconi, R.; Comelli, F. *Chim. Ind.* **1985**, *67*, 683.
(3) Francesconi, R.; Castellari, C.; Arcelli, A.; Comelli, F. *Can. J. Chem. Eng.* **1980**, *58*, 113.
(4) Monk, P.; Wadso, I. *Acta Chem. Scand.* **1968**, *30*, 352.
(5) Francesconi, R.; Comelli, F. *J. Chem. Eng. Data* **1985**, *30*, 352.
(6) Grolier, J. P. E.; Inglese, A. *Int. Data Ser., Ser. A* **1985**, 10.
(7) Weissberger, A. *Organic Solvents*, 2nd ed.; Interscience: New York, 1955; Vol. VII.
(8) *International Critical Tables*; McGraw-Hill: New York, 1928; Vol. 3, p 27.
(9) Nagata, I. *Int. Data Ser., Ser. A* **1984**, 75-77.
(10) Emmerich, W.; Inglese, A.; Grolier, J.-P. E.; Kehiaian, H. V. *J. Chem. Thermodyn.* **1982**, *14*, 33.
(11) Comelli, F.; Lunelli, B.; Francesconi, R. *J. Chem. Eng. Data* **1988**, *33*, 84.

Received for review June 1, 1988. Revised February 8, 1989. Accepted March 13, 1989. This work was supported by Ministero Pubblica Istruzione, Roma, Italy.

Solubilities of *n*-Octadecane, Phenanthrene, and *n*-Octadecane/Phenanthrene Mixtures in Supercritical Propane at 390 and 420 K and Pressures to 60 bar

Dimitrios Dimitrelis and John M. Prausnitz*

Materials and Chemical Sciences Division, Lawrence Berkeley Laboratory, and Department of Chemical Engineering, University of California, Berkeley, California 94720

Solubility data were obtained for *n*-octadecane, phenanthrene, and a nearly equimolar *n*-octadecane/phenanthrene mixture in supercritical propane. Solubilities were measured in a flow apparatus at 390 and 420 K over the pressure range 35–60 bar. The experimental data have been correlated using the perturbed-hard-chain equation of state. Agreement between experiment and correlation is good.

Introduction

Supercritical-fluid extraction has received wide attention during the past few years for potential application in the specialty-chemicals, pharmaceutical, and petroleum industries (*1*). At the center of this new technology lies enhanced solubility of the solute near the solvent's critical point. Experimental information on selected model systems is required to utilize molecular-thermodynamic models for representing the complex systems encountered in industrial applications.

Model systems using carbon dioxide or ethylene as the supercritical solvent have been studied extensively (*2–5*). However, only a few studies have reported data for systems where the gaseous solvent has a critical temperature significantly above that of carbon dioxide (304.2 K) (*6*, *7*). In this work we present solubilities of two model compounds (*n*-octadecane and phenanthrene) in supercritical propane.

Propane's critical point (369.8 K and 41.9 bar) makes it a suitable solvent for deasphalting processes in the petroleum industry. *n*-Octadecane and phenanthrene represent two classes of hydrocarbon compounds, aliphatic and aromatic, found in heavy fossil fuels. Both are liquids in the temperature range investigated in this work; both exhibit essentially identical vapor pressures within this temperature range.

Experimental Apparatus

Figure 1 shows a modified version of an apparatus described previously (*8*). Propane is pumped through the apparatus by a positive-displacement liquid pump from a cylinder. The desired pressure is adjusted by a back-pressure regulator. High-pressure propane reaches the desired temperature upon flowing through a heat exchanger inserted in a constant-temperature fluidized-sand bath. Propane then passes through a packed-bed cell where it equilibrates with the heavy hydrocarbon at measured temperature and pressure. The temperature of the saturated fluid leaving the packed bed is raised to approximately 150 deg above the bath temperature to avoid precipitation of the heavy hydrocarbons; the fluid is then expanded and directed through a heated gas-sampling valve to take samples intermittently as discussed below. Gas samples are analyzed in a gas chromatograph; the area of the peaks is measured by an electronic integrator and displayed on a chart recorder. Thermal cracking was insignificant; we ascertain the absence of cracking reactions in the equilibrium cell or the heated downstream portion of the equipment by monitoring the gas-chromatograph signal for extraneous peaks. Finally, the propane stream passes through a condenser where the heavy hydrocarbon precipitates. Subsequently, the pure-propane stream passes through a flowmeter where its cumulative volume is measured. The experimental procedure is automated once steady-state fluid flow is reached. Complete vaporization of the heavy hydrocarbon is signaled by a sharp decrease in the chromatogram peak area. To increase the rate of data acquisition, we use two flow systems in parallel.

When using a flow-solubility apparatus to study supercritical fluid-phase equilibria, it is necessary to exercise care when expanding from the experimental pressure to ambient pressure as required to facilitate downstream chemical or gravimetric

---

* Author to whom correspondence should be addressed

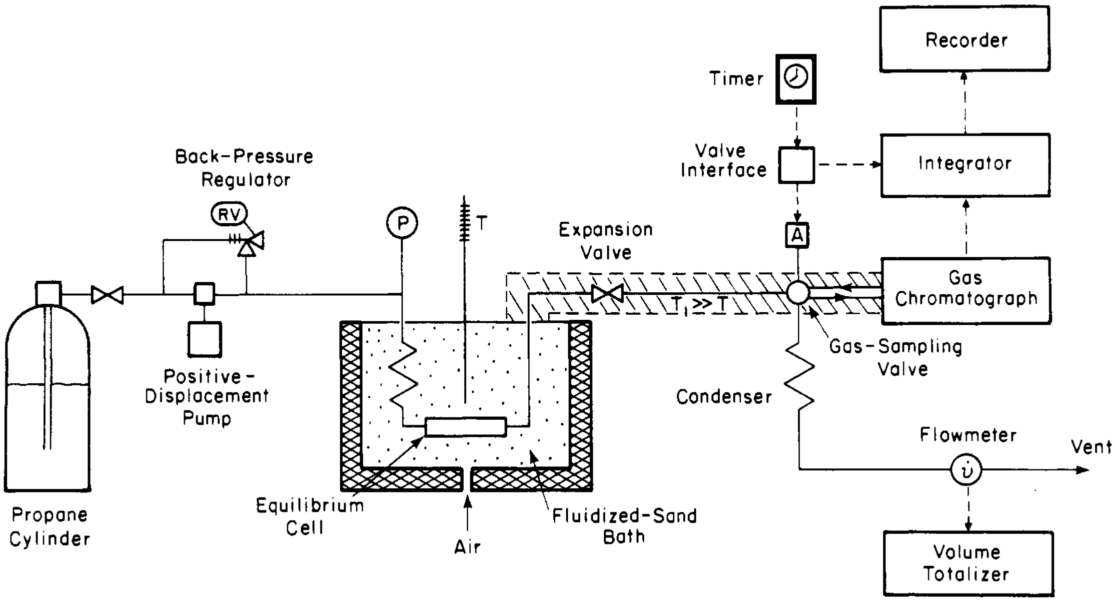

Figure 1. Apparatus for measuring the solubility of heavy hydrocarbons in supercritical propane.

analysis. Attention must be given toward solving two serious experimental problems. First, in the retrograde region, there is a solubility minimum at intermediate pressures for a given temperature. Since isothermal expansion may decrease the equilibrium solubility, the solute may precipitate. Therefore, it is necessary to heat the expansion valve to a temperature for which the equilibrium solubility minimum is greater than the measured solubility in the equilibrium cell.

Second, it is necessary to assure that, during the isobaric temperature increase between the equilibrium cell and the expansion valve, the solubility of the solute in the solvent increases monotonically. Otherwise, solute redeposition at some intermediate location can falsify the experimental results because the measured solubility will be assigned erroneously to the temperature of the equilibrium cell and not to the unknown temperature of that intermediate location. Other researchers (*2*, *5*) employ high linear gas velocity downstream of the equilibrium cell to avoid this problem by not allowing for establishment of thermodynamic equilibrium between the equilibrium cell and the expansion valve.

These two experimental problems encountered in the retrograde region dictate upper limits for the experimentally accessible ranges of temperature and pressure. Usually, the second difficulty is the more restrictive one, while the first depends on the temperature rating of the equipment downstream of the equilibrium cell. In this work, our measurements are restricted to those regions of the pressure-temperature phase space where downstream redeposition due to the above-stated limitations does not occur. When coupled with selected available experimental data, a molecular-thermodynamic model can provide guidance to determine these restricted regions. To be sure that no precipitation occurred between the equilibrium cell and the condensers, the mass balance between the weighted amount of loaded heavy hydrocarbons into the cell and the precipitated mass in the condensers was verified. Further, after completion of an experimental run, the temperature downstream of the equilibrium cell was raised by another 100 deg and the gas chromatograph was monitored to assure that no redeposited heavy hydrocarbons were emerging.

The lower limits for the temperature- and pressure-range window are set by the sensitivity of the analytical technique used to analyze the gas samples. In our work, since we used gas chromatography without an internal standard, we were able to analyze only samples with a solute mole fraction greater than 10^{-4}.

The liquid pump is an instrument minipump Model 396-31 from Laboratory Data Control. To avoid vaporization of propane, the pump head is cooled to 283 K. To prevent hydrate formation (*9*), which clogs the discharge valve of the pump, water traces are removed from the propane stream by a Matheson gas purifier Model 450 placed upstream of the pump. The discharge pressure is adjusted by a Model 31 back-pressure regulator from Circle Seal Controls. The pressure is measured with a Heise bourdon-tube pressure gauge calibrated against a dead-weight gauge.

The temperature of the fluidized-sand bath (Model SBS-4 by Techne) is controlled by a Thermotrol controller of Halikainen Instruments using a Model PR-11 resistance-thermometer probe (RTD) by Omega. The temperature uniformity within the working space of the bath is better than 0.5 K (*10*). The temperature uniformity across the equilibrium cells was verified (using multiple thermocouples) to be better than 0.2 K. The temperature is measured with an iron/constantan thermocouple whose reading is displayed on an Omega Trendicator Model 410, calibrated on the 1968 IPTS scale.

The packed-bed cells are made of stainless-steel tubes, 0.1 m in length and 5×10^{-3} m inner diameter. The solute is introduced into the cell in solid form at three evenly spaced points separated with a 60/80-mesh Chromosorb-P column support. The mass of the heavy hydrocarbon is determined by weighing the funnel (made of ultrathin weighing paper) with a Mettler mass balance Model HK 160 before and after loading.

A specially designed high-temperature, high-pressure expansion valve is used to expand the compressed-fluid mixture from the packed-bed cell so that the fluid can be sampled and metered. Details are presented elsewhere (*11*). The gas-sampling valve is a VALCO 10-port, high-temperature sampling valve with 5.7×10^{-7} m^3 sample loops. A 10-port valve with two sample loops is used such that the fluid streams from two different packed-bed equilibrium cells can be sampled alternatively. Sampling is automated by use of a VALCO digital valve interface, a VALCO two-position helical-drive air actuator, and a mechanical timer. A typical run lasts 1–2 days; samples are taken automatically every 30 min.

Gas samples are analyzed by use of a Perkin-Elmer Model 990 gas chromatograph with a hydrogen-flame ionization detector under isothermal, differential (compensated-mode) operation. The chromatographic column is a 2-m-long, 2.2×10^{-3} m inner diameter stainless-steel tube packed with a 3% OV-101 Chromosorb W-HP column support. The output from the

Table I. Solubility of Anthracene in Propane

T, K	P, bar	mol %
419.5	46.1	0.0351
419.5	48.3	0.0400
420.0	52.6	0.0478
419.6	56.3	0.0541

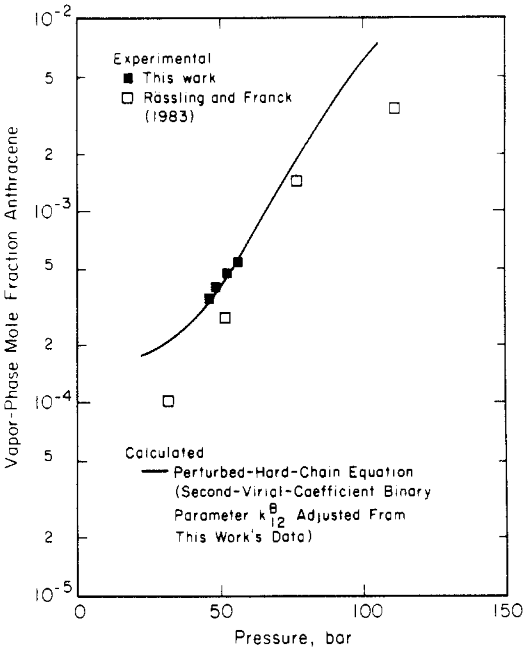

Figure 2. Calculated and experimental solubilities of anthracene in propane at 420 K.

gas chromatograph is measured and recorded by use of a Spectra-Physics single-channel integrator and displayed on a Honeywell strip-chart recorder.

The cumulative volume of propane is measured through integration of the propane flow over time by a Matheson mass flowmeter, Series 8100; the output signal is fed to a Totalizer Model 8122.

The results of the intermittent fluid-phase analysis are plotted against the corresponding cumulative propane volume (at standard temperature and pressure) having passed through the equilibrium cell. The solubility is obtained by using the equal-area data-reduction technique described elsewhere (*8*).

Materials

The propane cylinder was supplied by Matheson with full-length eductor tubes for liquid withdrawal. Propane was of CP grade with a 99.0% minimum purity in the liquid phase. The solutes were supplied by Aldrich. Purity was 98+% for anthracene, 97% for *n*-octadecane, and 98+% for phenanthrene.

The accuracy in reported temperature is better than ±0.15 K; the accuracy in reported pressure is better than ±1% over the entire range. Finally, the accuracy in the reported solubility is better than ±5%.

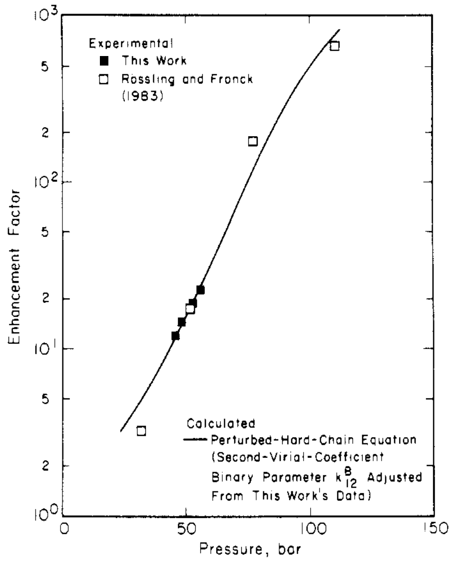

Figure 3. Calculated and experimental enhancement factor for anthracene in propane at 420 K.

Table II. Solubility of *n*-Octadecane in Propane

T, K	P, bar	mol %
389.9	36.1	0.0257
389.9	40.3	0.0408
390.0	46.1	0.0729
419.5	45.9	0.110
419.6	52.5	0.160
419.6	53.0	0.174
419.6	60.7	0.302

Table III. Solubility of Phenanthrene in Propane

T, K	P, bar	mol %
389.7	36.3	0.0319
390.0	40.7	0.0433
390.0	44.7	0.0630
419.0	45.7	0.0901
419.1	53.5	0.136
419.1	58.9	0.189

Table IV. Solubility of a Nearly Equimolar Mixture of *n*-Octadecane/Phenanthrene in Propane

T, K	P, bar	mol %
388.7	42.7	0.0676
419.7	54.5	0.227

Experimental Results

To check the apparatus, solubility data were obtained for anthracene. Table I presents the solubility of anthracene in propane at 420 K. Figure 2 compares our measurements with those reported by Rössling and Franck (*6*), who used a static apparatus. The solid line shows a correlation of our measurements using the perturbed-hard-chain equation as described below. Our data are correlated well within the 5% experimental accuracy. The data by Rössling and Franck (*6*) lie in a 125%-rms-deviation window from the calculated solubility curve. The discrepancy between the two data sets is larger than the estimated experimental error.

Figure 3 shows the enhancement factor for anthracene as a function of pressure. The enhancement factor is defined as the ratio of the solute's partial pressure over its vapor pressure at given temperature and pressure. The data of Rössling and Franck are normalized using their own vapor-pressure measurements, while our data are normalized using the sublimation-pressure equation reported in API Publication 709 (*12*). The resulting enhancement factors for the two sets of measurements are within the reported experimental error. Therefore, the difference between the two sets of solubility data is not larger than the variation in the sublimation pressure reported in the literature for anthracene.

Tables II and III present solubilities of *n*-octadecane and phenanthrene, respectively, in supercritical propane at 390 and 420 K and pressures to 60 bar. Table IV presents the solubility of a *n*-octadecane/phenanthrene mixture in supercritical propane. The composition of the liquid phase on a propane-free basis is 46 mol % phenanthrene and 54 mol % *n*-octadecane.

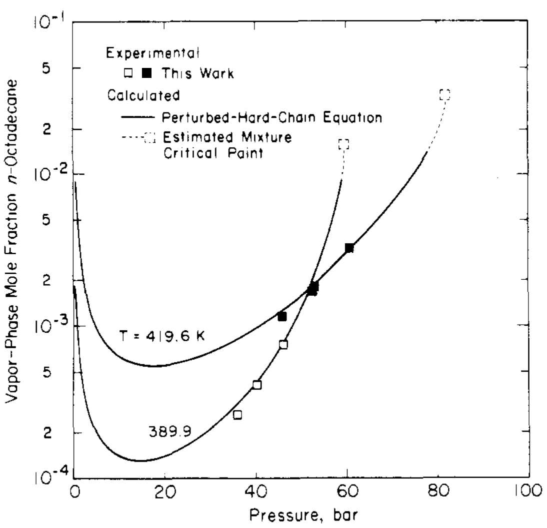

Figure 4. Calculated and experimental solubilities of *n*-octadecane in propane.

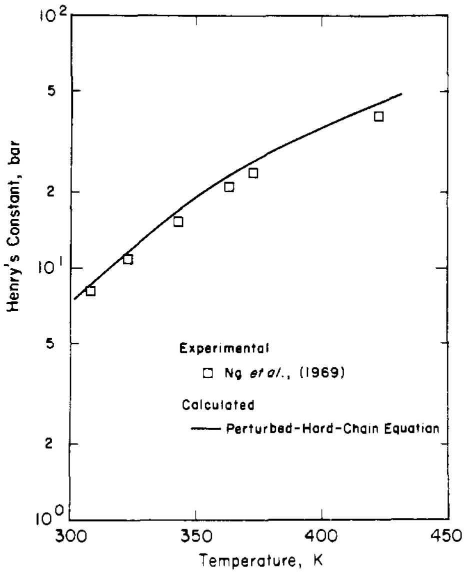

Figure 5. Predicted and experimental Henry's constant for propane in *n*-octadecane (binary parameter k^B_{12} from solubility data for *n*-octadecane in propane).

The tabulated vapor-phase mole fraction of the heavies is the measured total sum of the *n*-octadecane and phenanthrene mole fraction in the vapor phase.

Data Correlation and Discussion

We used the perturbed-hard-chain (PHC) equation of state (*13*, *14*) to correlate our experimental results. For *n*-octadecane and phenanthrene, we used the parameters reported by Cotterman et al. (*13*).

Since our measurements are near propane's critical point, we adjusted the equation-of-state parameters for propane to represent better the properties of propane in its near-critical region. We used $T^* = 245.69$ K, $v^* = 4.316 \times 10^{-5}$ m^3/mol, and $c = 1.51$.

As discussed elsewhere (*11*), the choice of equation-of-state parameters has an effect on mixture calculations near the solvent's critical point. Overprediction of the solvent's critical temperature and pressure (even by a few degrees or a few bars) can adversely affect solubility calculations in the solvent's near-critical region. Therefore, the equation-of-state parameters for propane were obtained by preferentially weighting pure-component vapor-pressure data near its critical point and by requiring that the critical isotherm goes through the critical point at the experimentally observed critical pressure and temperature.

Figure 4 shows calculated and experimental results for the solubility of *n*-octadecane in propane. Using only one adjustable binary parameter $k^B_{12} = -0.06$, we were able to correlate our measurements for both isotherms over the entire pressure range within 5% rms deviation. Dense-fluid parameter k_{12} was set to zero. The model correctly predicts that the propane/*n*-octadecane mixtures conform to type D phase behavior according to the classification of Kohn et al. (*15*).

Figure 5 shows calculated and experimental (*16*) Henry's constants for propane in *n*-octadecane. The calculations are performed using the binary parameter obtained from the solubility measurements. The measurements are correlated within experimental error over a wide range of temperature. Thus, the gas-phase solubility data appear to be consistent with the liquid-phase solubility data.

Figure 6 shows calculated and experimental results for the solubility of phenanthrene in propane. Without any binary parameter, the equation correlates the experimental data within 8% rms deviation. The equation of state predicts that at the lower temperature there is liquid–liquid immiscibility between a

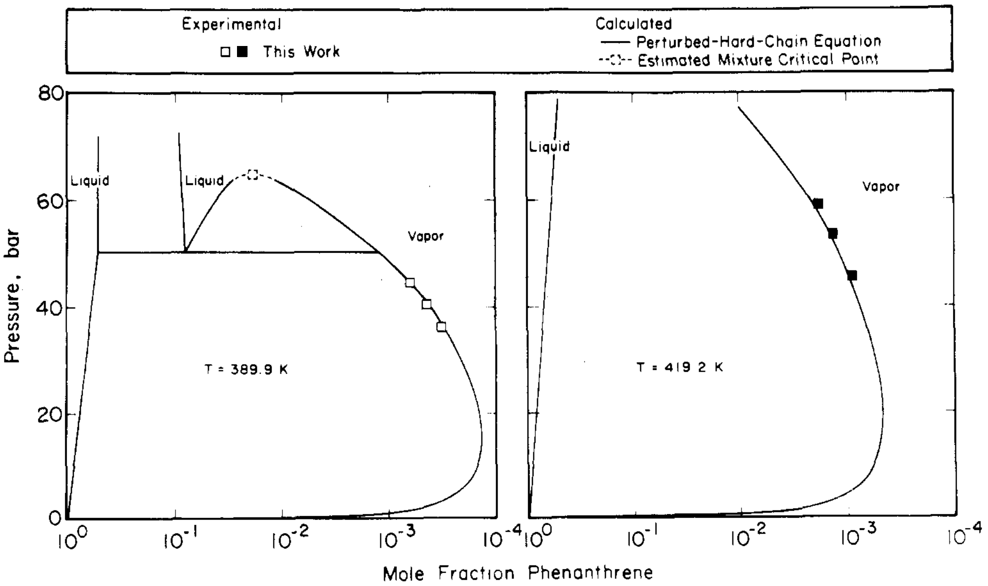

Figure 6. Calculated and experimental phase equilibria for propane/phenanthrene.

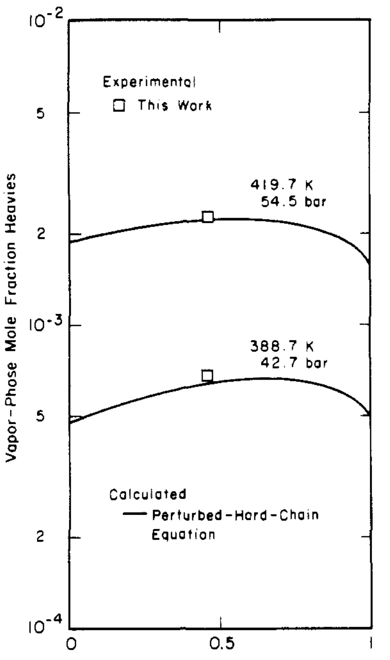

Figure 7. Calculated and experimental solubilities for *n*-octadecane/phenanthrene mixture in propane.

phenanthrene-rich and a propane-rich liquid phase. As discussed by Kohn et al. (*15*), such phase behavior is common for binary mixtures for which the triple point of the heavier component (the freezing point of phenanthrene is 373.7 K) is slightly higher than the critical temperature of the lighter component.

Figure 7 shows calculated and experimental solubilities of *n*-octadecane/phenanthrene mixtures in propane at two different temperatures and pressures. The liquid-phase composition on the abscissa is on a propane-free basis. The calculated solubilities are the sum of the vapor-phase mole fractions for *n*-octadecane and phenanthrene. For the two-solute system, there is an enhancement of the overall solubility compared with the solubilities of the individual heavy hydrocarbons.

The results indicate that calculations using the binary constants (propane/*n*-octadecane and propane/phenanthrene) do not correlate the vapor-phase composition for this ternary mixture. It is also necessary to include a binary constant for the liquid phase containing the two heavy hydrocarbons. Because no experimental information is available for *n*-octadecane/phenanthrene vapor-liquid equilibria, we assume that the dense-fluid parameter k_{12} for *n*-octadecane/phenanthrene is similar to that for *n*-hexadecane/phenanthrene. Correlation of vapor-liquid equilibria data for *n*-hexadecane/phenanthrene (*17*) using the PHC equation gives k_{12} equal to 0.03. The solid line in Figure 7 shows calculated results using one interaction parameter per binary. These calculated results correlate the measured data within a 5% rms deviation.

Figure 8 presents the selectivity of propane for an equimolar *n*-octadecane/phenanthrene mixture. Selectivity is defined as the ratio of equilibrium *K* factors for phenanthrene and *n*-octadecane. Propane is slightly more selective for phenanthrene than for *n*-octadecane. This selectivity difference cannot be attributed to vapor-pressure effects since the vapor pressures of the two model compounds are essentially the same over the temperature range investigated. The observed selectivity may be related to weak interactions between the quadrupole moment of phenanthrene and weak dipole moment of propane.

At the lower temperature, the selectivity decreases initially with pressure but then increases as the pressure approaches the mixture critical point for the binary systems. At the higher temperature we observe an azeotrope.

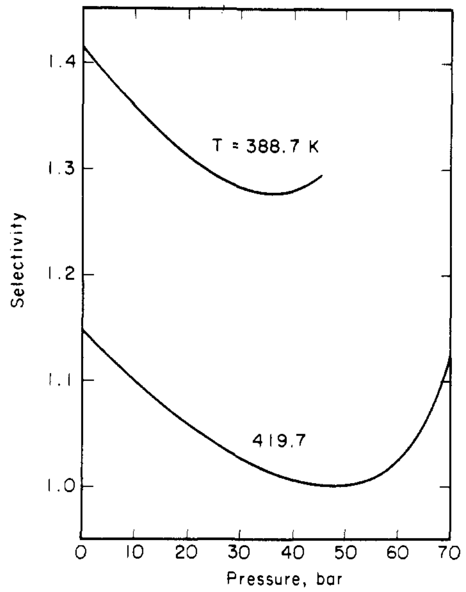

Figure 8. Calculated solubility ratio (selectivity) for an equimolar *n*-octadecane/phenanthrene liquid mixture in propane.

Propane appears to be more selective for aromatic than for aliphatic hydrocarbons with the same vapor pressure. (A different conclusion may result when selectivity is measured for aromatic and aliphatic hydrocarbons with the same carbon number or with the same molecular weight (*18*).) Our results confirm those of previous work on the selectivity of propane for a continuous oil mixture containing saturated and aromatic hydrocarbons (*18*). Propane is a more selective solvent at temperatures near its critical; at higher temperatures, selectivity decreases while solvent power increases.

Glossary

c	Prigogine's parameter
k	binary interaction parameter
PHC	perturbed-hard-chain equation of state
T	temperature
v	molar volume

Superscripts

B	second virial coefficient
*	perturbed-hard-chain equation-of-state parameters

Subscripts

ij	interaction between component *i* and component *j*

Registry No. *n*-Octadecane, 593-45-3; phenanthrene, 85-01-8; propane, 74-98-6.

Literature Cited

(1) Paulaitis, M. E.; Krukonis, V. J.; Kurnik, R. T.; Reid, R. C. Supercritical Fluid Extraction. *Rev. Chem. Eng.* **1983**, *1*, 179.
(2) Kurnik, R. T.; Holla, S. J.; Reid, R. C. Solubility of Solids in Supercritical Carbon Dioxide and Ethylene. *J. Chem. Eng. Data* **1981**, *26*, 47.
(3) McHugh, M.; Paulaitis, M. E. Solid Solubilities of Naphthalene and Biphenyl in Supercritical Carbon Dioxide. *J. Chem. Eng. Data* **1980**, *25*, 326.
(4) Dobbs, J. M.; Wong, J. M.; Johnston, K. P. Nonpolar Co-Solvents for Solubility Enhancement in Supercritical-Fluid Carbon Dioxide. *J. Chem. Eng. Data* **1986**, *31*, 303.
(5) Johnston, K. P.; Zigler, D. H.; Eckert, C. A. Solubilities of Hydrocarbon Solids in Supercritical Fluids. The Augmented van der Waals Treatment. *Ind. Eng. Chem. Fundam.* **1982**, *21*, 191.
(6) Rössling, G. L.; Franck, E. U. Solubility of Anthracene in Dense Gases and Liquids to 200 C and 2000 bar. *Ber. Bunsen-Ges. Phys. Chem.* **1983**, *87*, 882.
(7) Yonker, C. R.; Smith, R. D. Solubilities of Caffeine and Theophylline in Supercritical Ammonia. *Fluid Phase Equilib.* **1985**, *22*, 175.
(8) Monge, A.; Prausnitz, J. M. An Experimental Method for Measuring Solubilities of Heavy-Fossil Fuel Fractions in Compressed Gases to 100 bar and 300 C. In *Chemical Engineering at Supercritical Fluid Conditions*; Paulaitis, M. E., Penninger, J. M. L., Gray, R. D., Jr., David-

son, P., Eds.; Ann Arbor Science: Ann Arbor, MI 1983; pp 159-171.
(9) Anderson, F. E.; Prausnitz, J. M. Inhibition of Gas Hydrates by Methanol. *AIChE J.* **1986**, *32*, 1321.
(10) Techne Incorporated. Tecam Temperature Calibration Baths, Catalog no. 301/302, Princeton, NJ, 1982.
(11) Dimitrelis, D. Phase Equilibria for Supercritical Fluid Extraction. Doctoral Dissertation, University of California, Berkeley, CA, 1989.
(12) *Anthracene and Phenanthrene*; API Monograph Series; API Publication 708; American Petroleum Institute: Washington, DC, 1979.
(13) Cotterman, R. L.; Schwartz, B. J.; Prausnitz, J. M. Molecular Thermodynamics for Fluids at Low and High Densities. Part I: Pure Fluids Containing Small or Large Molecules. *AIChE J.* **1986**, *32*, 1787.
(14) Cotterman, R. L.; Prausnitz, J. M. Molecular Thermodynamics for Fluids at Low and High Densities. Part II: Phase Equilibria for Mixtures Containing Components with Large Differences in Molecular Size or Potential Energy. *AIChE J.* **1986**, *32*, 1799.
(15) Kohn, J. P.; Luks, K. D.; Kulkarni, A. J. Solubility of Hydrocarbons in Cryogenic NGL and LNG. *Proceedings of the Fifty-Third Annual Convention*; Gas Processors Association: Tulsa, OK, 1974; pp 21-25.
(16) Ng, S.; Harris, H. G.; Prausnitz, J. M. Henry's Constants for Methane, Ethane, Ethylene, Propane, and Propylene in Octadecane, Eicosane, and Docosane. *J. Chem. Eng. Data* **1969**, *14*, 482.
(17) McMakin, I. E., Jr.; van Winkle, M. Vapor-Liquid Equilibrium of *n*-Hexadecane-Bibenzyl-Phenanthrene System at 100 mm of Mercury Absolute. *J. Chem. Eng. Data* **1962**, *7*, 9.
(18) Tietz, M.; Dimitrelis, D.; Prausnitz, J. M. The Effect of an Aqueous Entrainer on Phase Equilibria for Supercritical Extraction of Heavy Fossel Fuels with Propane. Report 22471; Lawrence Berkeley Laboratory, University of California: Berkeley, CA, November, 1986.

Received for review July 11, 1988. Accepted January 27, 1989. This work was supported by the Director, Office of Energy Research, Office of Basic Energy Sciences, Chemical Sciences Division of the U.S. Department of Energy under Contract No. DE-AC03-76SF00098. For additional financial support we are also grateful to Exxon Research and Engineering Company, to the donors of the Petroleum Research Fund, administered by the American Chemical Society, and to the National Science Foundation.

High-Pressure Vapor–Liquid Equilibria Involving Mixtures of Nitrogen, Carbon Dioxide, and *n*-Butane

Steven K. Shibata[†] **and Stanley I. Sandler***

Department of Chemical Engineering, University of Delaware, Newark, Delaware 19716

A new high-pressure vapor–liquid equilibrium apparatus has been constructed with the capability of measuring the compositions and densities of the coexisting equilibrium phases at constant temperature and/or pressure. This apparatus was tested with the carbon dioxide + *n*-butane system with excellent agreement observed between our results and previously published data. Data are also reported for the nitrogen + *n*-butane system and the previously unmeasured nitrogen + carbon dioxide + *n*-butane system. These data were modeled with the Peng–Robinson equation of state. Excellent fits were obtained for the compositions in the carbon dioxide + *n*-butane system, but a poor fit was obtained for the nitrogen + *n*-butane data. The ability of the Peng–Robinson equation of state to accurately predict the phase behavior of the ternary mixture is dependent on the fits of the binary data, and therefore the ternary data are also not fit well. In all cases the liquid densities are poorly predicted with the Peng–Robinson equation of state.

Introduction

Petroleum reservoir management, enhanced oil recovery, and separation processes in the oil and gas industries all involve modeling phase behavior of multicomponent mixtures consisting of hydrocarbons, carbon dioxide, nitrogen, and other nonhydrocarbons. The motivation for this research is to obtain experimental data on these systems and to utilize these data in evaluating equations of state and their mixing rules. By simultaneously determining both the compositions and the densities of the coexisting phases, equations of states and their mixing rules can be more stringently tested than with composition data alone. In addition, correlations of the binary data are used to predict our ternary data to test the premise that the behavior of multicomponent systems can be accurately predicted from data for binary systems.

Equipment

The new apparatus is a double-recirculation cell with a maximum temperature and pressure of 300 °F and 5000 psia, respectively. The key components of the apparatus are a visual cell, recirculation pumps, and the density meters. As shown in Figure 1, the center of the apparatus is a 100-cm^3 through-windowed cell manufactured by Ruska. This cell has ports in the side, top, and bottom. Modified Ruska fittings in the top and bottom ports allow a countercurrent flow configuration in the cell with the liquid pouring into the vapor and the vapor bubbling up through the liquid. The side port is used for temperature measurement.

Recirculation is the result of two magnetic pumps (*1*); each pump is driven mechanically with ring magnets surrounding the barrel containing the piston. The magnets are supported within a carriage assembly attached to a small steel cable, which passes through the roof of the oven. No thermal disturbances were created by this arrangement since the motors driving the cables are located outside of the controlled temperature bath.

The last major component in the equipment is the Mettler Paar vibrating-tube density meters. The density meters consist of a digital readout box [DMA 60] and two vibrating-tube assemblies [DMA 512], one for each recirculation loop. For our application, the vibrating tube and the stabilizing block were separated from the sensitive electronics, because the electronics could not withstand the temperatures to which the vibrating tubes were subject. Calibration runs for each tube were made with an evacuated tube and a tube filled with distilled water, since this range of the calibration points bracketed all experimental densities. These density calibration constants are temperature dependent and therefore were determined at each temperature of interest and were checked periodically.

A double-recirculation, countercurrent flow configuration was used since this choice allowed measuring the phase densities of the recirculating phases. The schematic diagram of the apparatus is shown in Figure 1. Each recirculation loop contains a density tube, magnetic recirculation pump, and a set of sampling valves. Constant temperatures are maintained by enclosing the entire system in a Blue M oven [POM7-136C-3]. We operated the oven under manual control so as to minimize

---

[†] Present address: E. I. du Pont de Nemours & Company, Technical Group, Seaford, DE 19973.

* Author to whom correspondence should be addressed.

0021-9568/89/1734-0291$01.50/0